

ECCOMAS (ECCM-ECFD) 2018 conference, Glasgow, 11-15 June 2018

Wall-resolved and wall-modeled ILES based on high-order DG

Ralf Hartmann

14 June 2018



Knowledge for Tomorrow



Overview

1. DG discretization of
 - flow equations
 - integral quantities and
 - local quantities
2. Discretization settings and results/examples for
 - RANS
 - ILES
3. Wall-modelled ILES (WM-ILES)
 - Approach
 - Results



Discretization of equations, integral and local quantities

Discretization of flow equations:

$$\int_{\Omega} (-\mathcal{F}^c(\mathbf{u}_h) + \mathcal{F}^v(\mathbf{u}_h, \nabla_h \mathbf{u}_h)) : \nabla_h \mathbf{v}_h \, d\mathbf{x} + \dots + \int_{\Gamma} (\hat{\mathbf{h}}_{\Gamma,h} - \hat{\underline{\sigma}}_{\Gamma,h} \mathbf{n}) \cdot \mathbf{v}_h \, ds$$

Adjoint consistent discretization of **integral** quantities (drag, lift coefficients):

$$J(\mathbf{u}) = \int_{\Gamma_w} (\rho \mathbf{n} - \underline{\tau} \mathbf{n}) \cdot \boldsymbol{\psi} \, ds, \quad J_h(\mathbf{u}_h) = \int_{\Gamma_w} (\hat{\mathbf{h}}_{\Gamma,h} - \hat{\underline{\sigma}}_{\Gamma,h} \mathbf{n}) \cdot \tilde{\boldsymbol{\psi}} \, ds.$$

Adjoint consistent discretization of **local** quantities (surface pressure, skin friction)

$$c_p(\mathbf{u}) = \frac{p(\mathbf{u}) - p_{\infty}}{\frac{1}{2} \rho_{\infty} v_{\infty}^2}, \quad c_{p,h}(\mathbf{u}_h) = \frac{\hat{\mathbf{h}}_{\Gamma,h} \cdot \tilde{\mathbf{n}} - p_{\infty}}{\frac{1}{2} \rho_{\infty} v_{\infty}^2},$$

$$c_f(\mathbf{u}, \nabla \mathbf{u}) = \frac{\tau_w(\mathbf{u}, \nabla \mathbf{u})}{\frac{1}{2} \rho_{\infty} v_{\infty}^2}, \quad c_{f,h}(\mathbf{u}_h, \nabla \mathbf{u}_h) = -\frac{(\hat{\underline{\sigma}}_{\Gamma,h} \mathbf{n}) \cdot \tilde{\mathbf{t}}}{\frac{1}{2} \rho_{\infty} v_{\infty}^2},$$

with $\tilde{\mathbf{n}} = (0, n_1, n_2, 0)^{\top}$ for the normal vector $\mathbf{n} = (n_1, n_2)^{\top}$,
and $\tilde{\mathbf{t}} = (0, t_1, t_2, 0)^{\top}$ for the tangential vector $\mathbf{t} = (t_1, t_2)^{\top}$.

Hartmann, Leicht: JCP 300, 754-778, 2015



Computational/meshing challenge

4th Int. Workshop on High-Order CFD Meth.

DLR-F11 high lift configuration

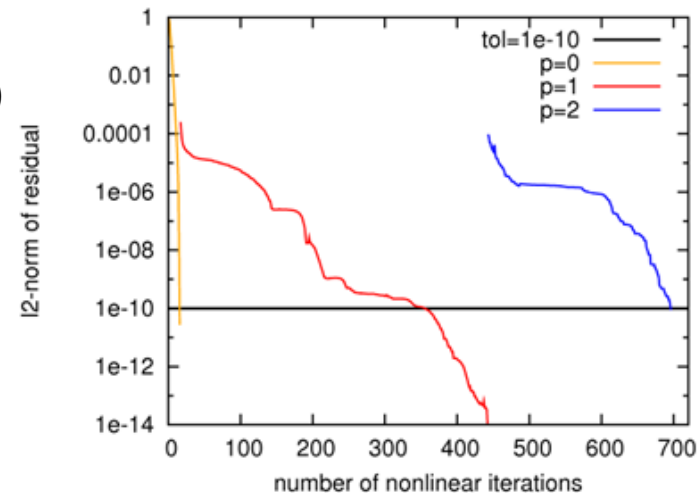
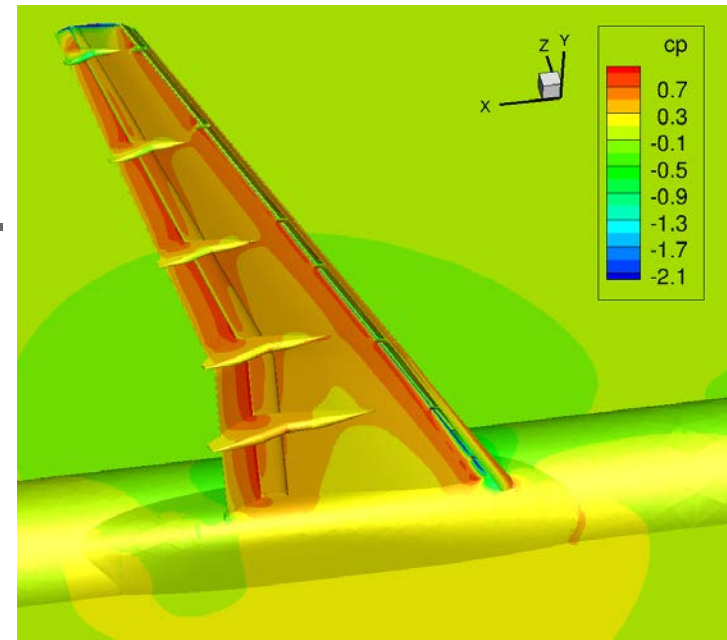
- Config 4 incl. slat tracks and flap track fairings
- Mach=0.175, $Re=15.1 \times 10^6$, $\alpha=7.0^\circ$
- Fully turbulent (**RANS with Wilcox-k ω model**)

Grid (by Harlan McMorris, CentaurSoft):

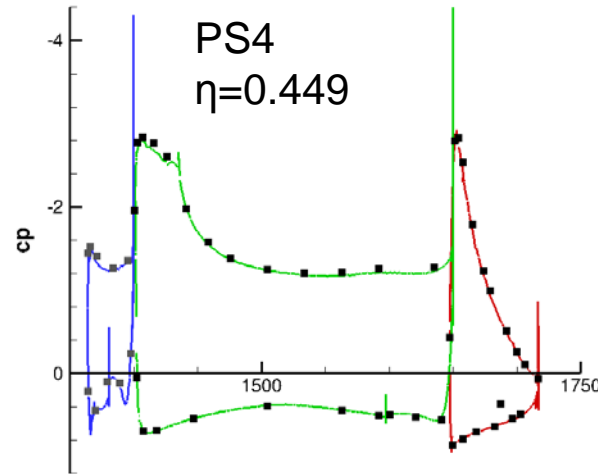
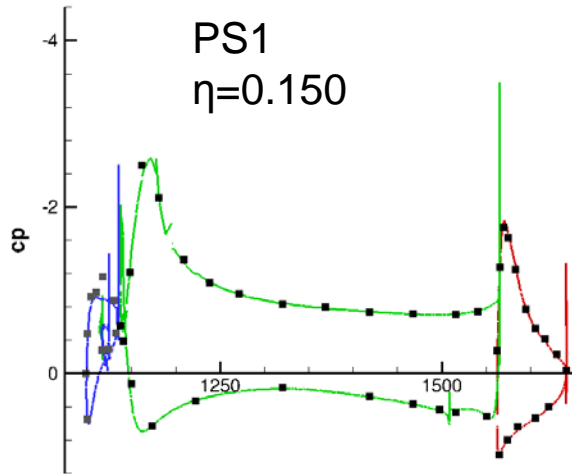
- Quadratic curved grid (Centaur)
- Hybrid grid (with prisms, pyramids and tetrahedra)
- 3.52×10^6 elements

Flow solver:

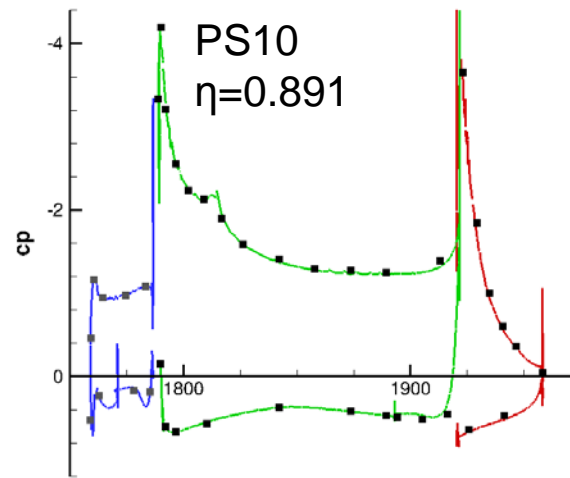
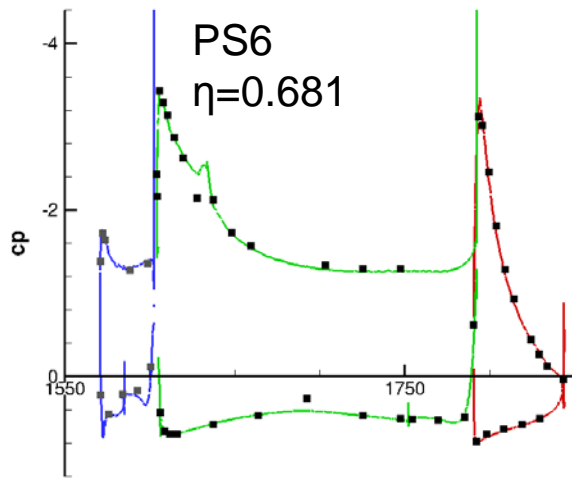
- PADGE solver, fully implicit solver (no multigrid)
- $p=0, 1, 2$ ($3.5, 14.1, 35.2 \times 10^6$ DoFs/eqn)
- Convergence of nonlinear residual below $1e-10$



The DLR-F11 high lift configuration: Results



DLR-F11, Config 4
Mach=0.175
Re=15.1x10⁶
alpha=7.0°
RANS Wilcox-kw
p=2: 35.2x10⁶ DoFs/eqn



	C_L	C_D	C_M
Exp.	1.9270	0.1615	-0.5390
TAU*	1.8794	0.1681	-0.5647
	-2.5%	+4.1%	-4.8%
PADGE	1.8781	0.1649	-0.5704
	-2.5%	+2.1%	-5.8%

* Rudnik, Melber(SAO)
HiLiftPW-2, 2013

Hartmann, McMorris, Leicht: ECCOMAS 2016



Discretization details: RANS vs. ILES

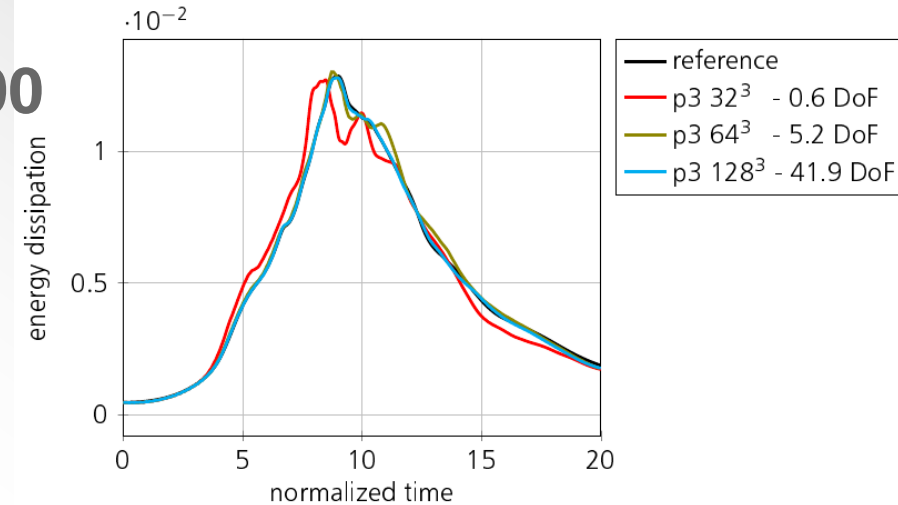
	RANS	ILES
Convective numerical flux	Roe with entropy fix	Roe without entropy fix
BR2 constant (on hexes)	6	2
DG basis functions [difference due to different flow solvers]	parametric	non-parametric



Taylor Green Vortex at Re=1600

DG, $p=3$ on 64^3 mesh,
 Comparison explicit vs. implicit RK
 ERK vs. SDIRK

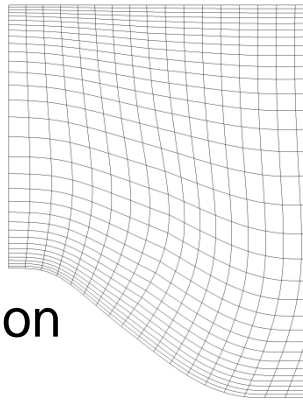
[Single coefficient diagonally implicit Runge-Kutta]



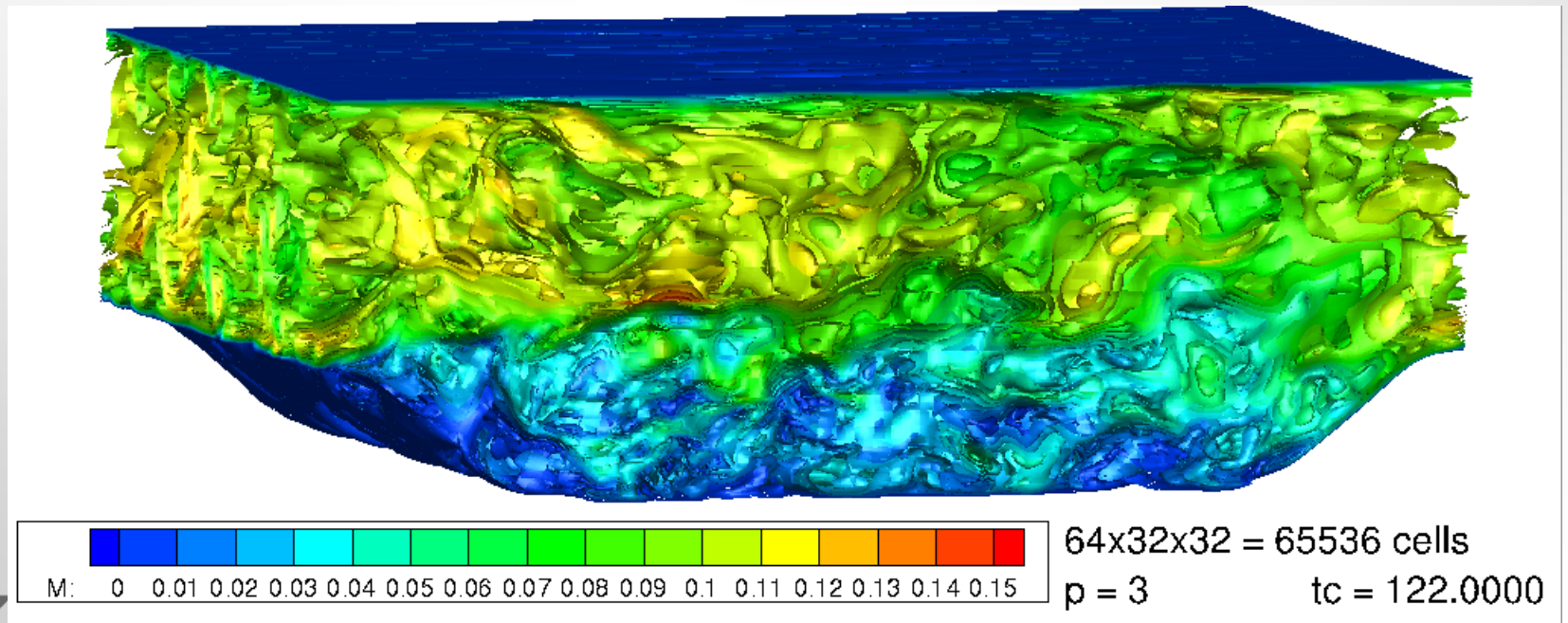
Scheme	t. step size	Run time	Note
ERK-4	0.001	1.0	reference
SDIRK-4	0.1	20.1	baseline
		1.3	freeze Jacobian for 1 time step, tol = 10^{-12}
		0.5	freeze Jac. for 1 time step, tol = 10^{-4}
		0.4	freeze Jac. for 2 time steps, tol = 10^{-4} („optimized“)
ESDIRK-3	0.05	0.8	„optimized“
ESDIRK-2	0.025	1.3	„optimized“

ILES for the 2D Periodic Hill test case at $Re_b=2800$

Quadratic grid
 64x32x32 elem.
 Global p-adaptation
 ERK-4

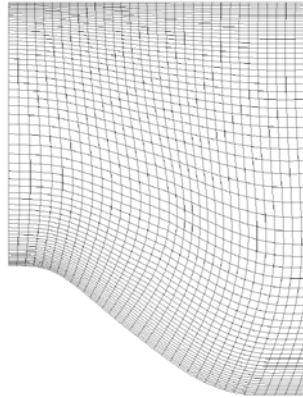


p	DoFs/eqn	tc	dtc	#steps
0	66 K	0 - 2	2e-4	10 K
1	262 K	2 - 32	1e-4	300 K
2	656 K	32 - 62	5e-5	600 K
3	1.3 M	62 - 122	3.33e-5	1.8 M



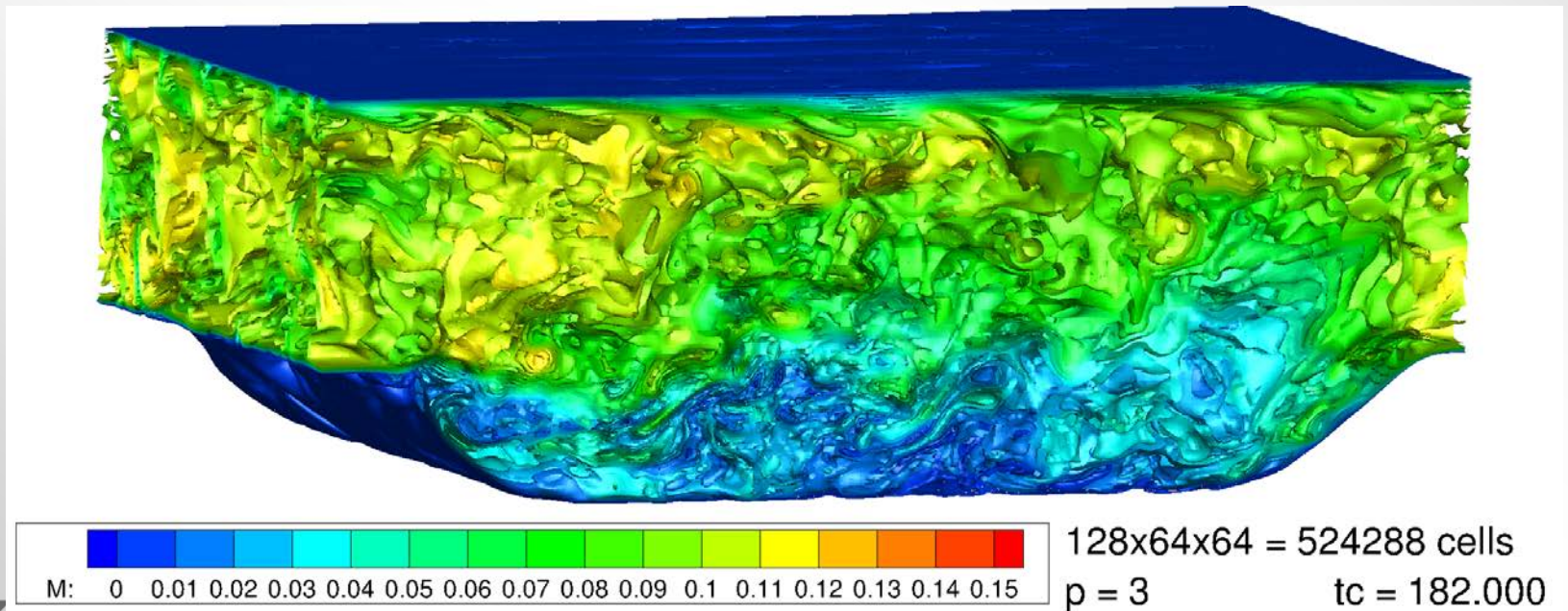
ILES for the 2D Periodic Hill test case at $Re_b=2800$

After global
h-refinement:

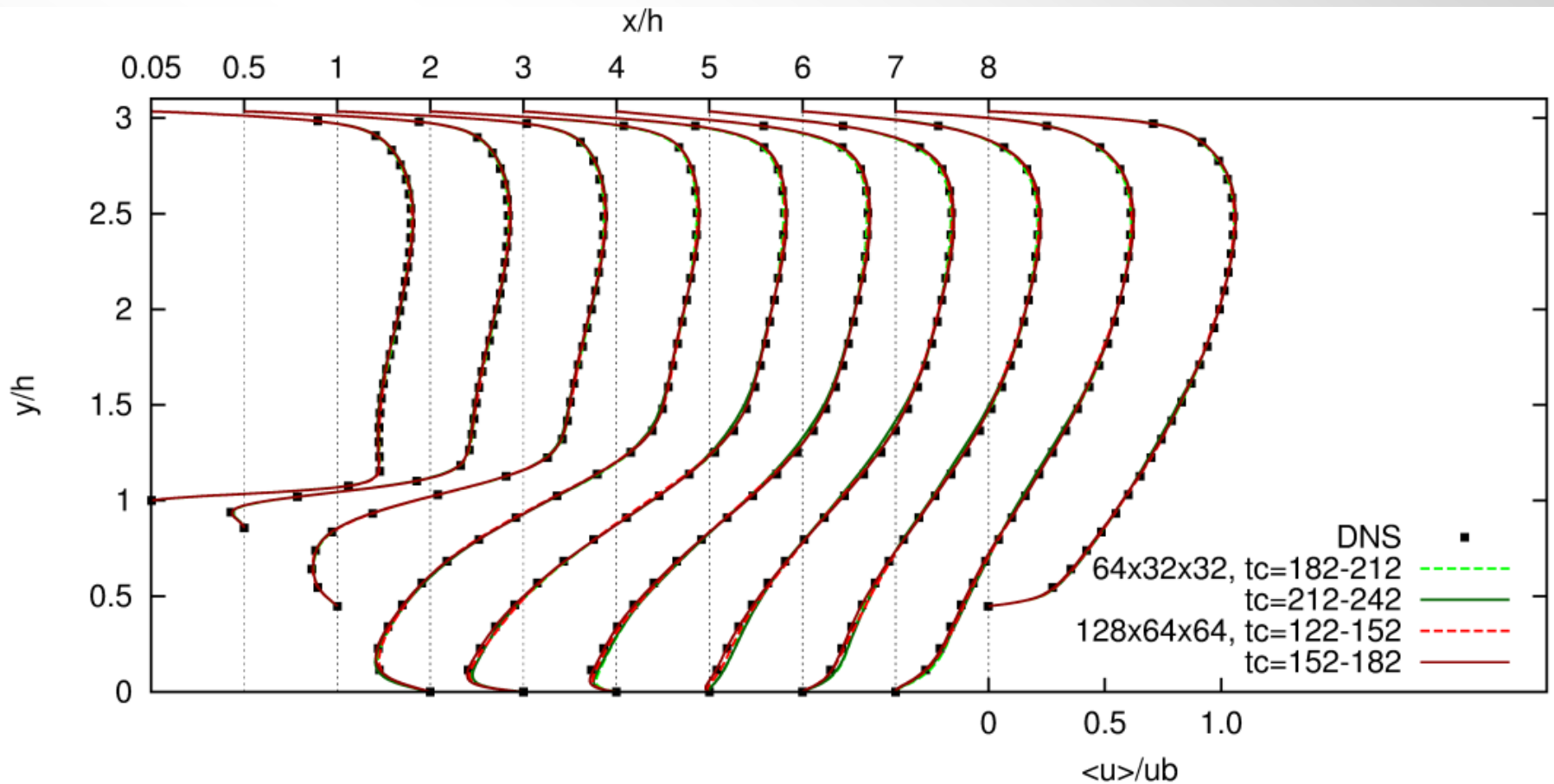


Quadratic mesh
128x64x64 elem.
SDIRK-4

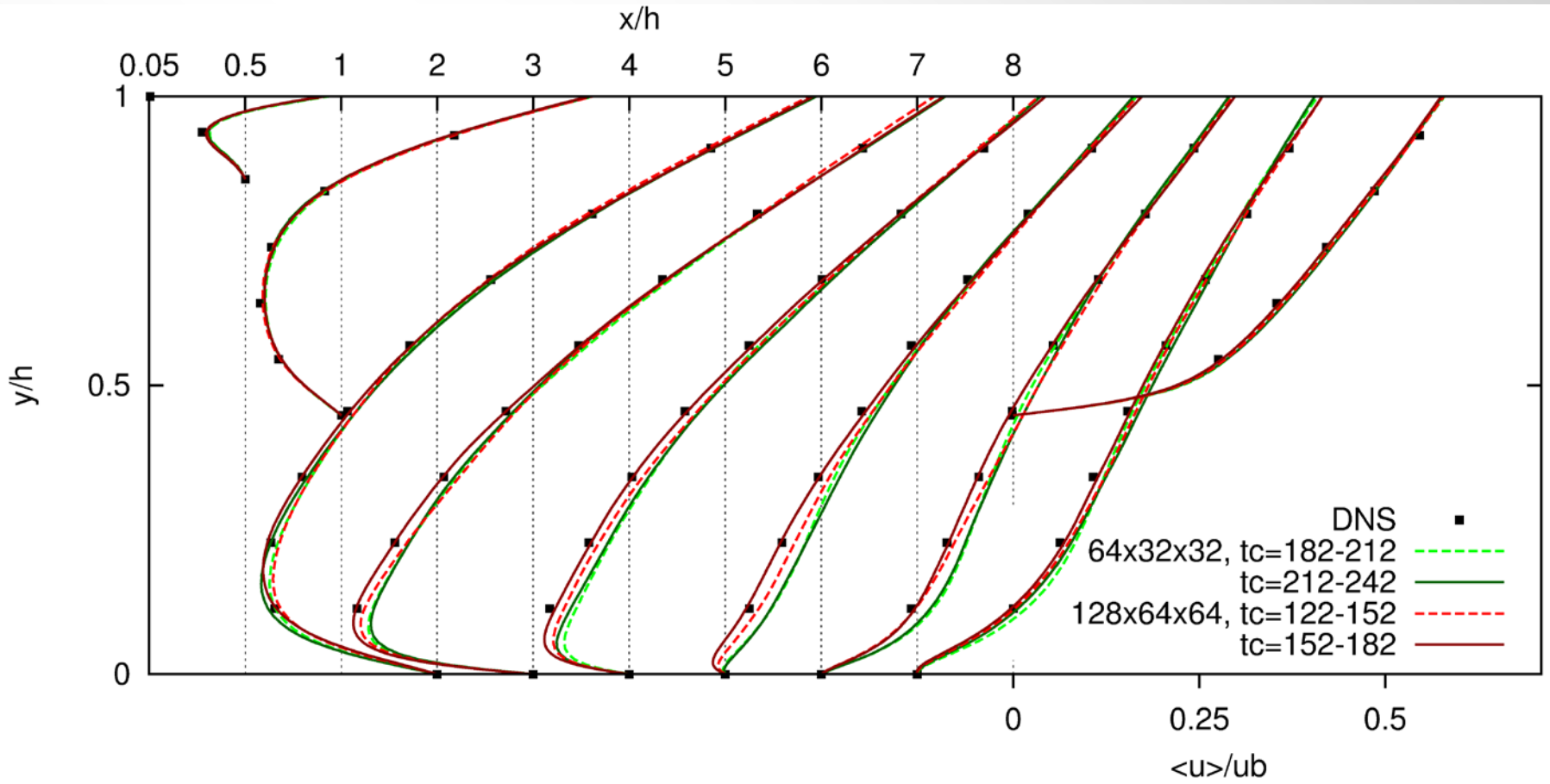
p	DoFs/eqn	tc	dtc	#steps
3	10.5 M	122 - 182	1.66e-3	36000



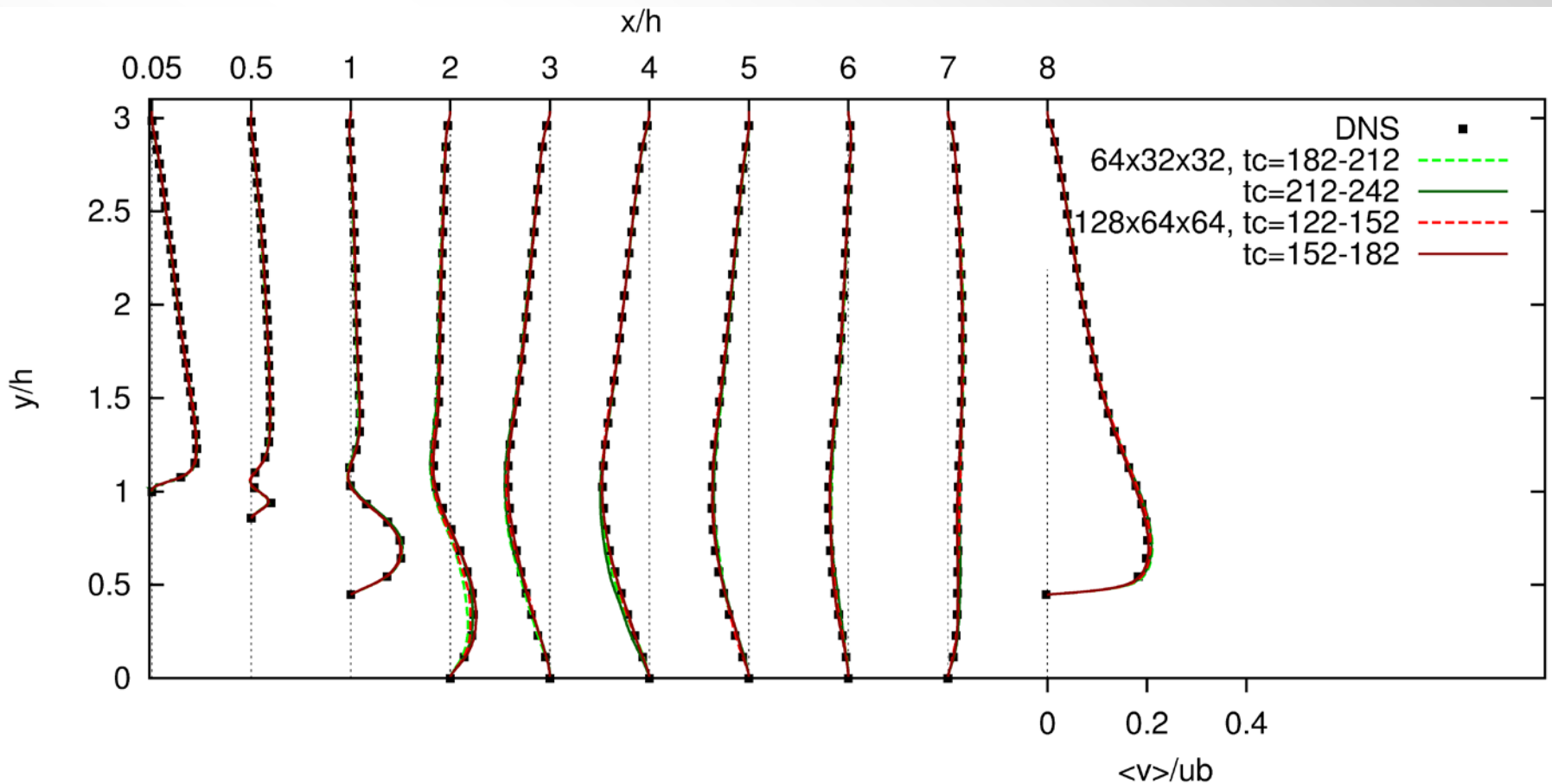
ILES for the 2D Periodic Hill test case at $Re_b=2800$



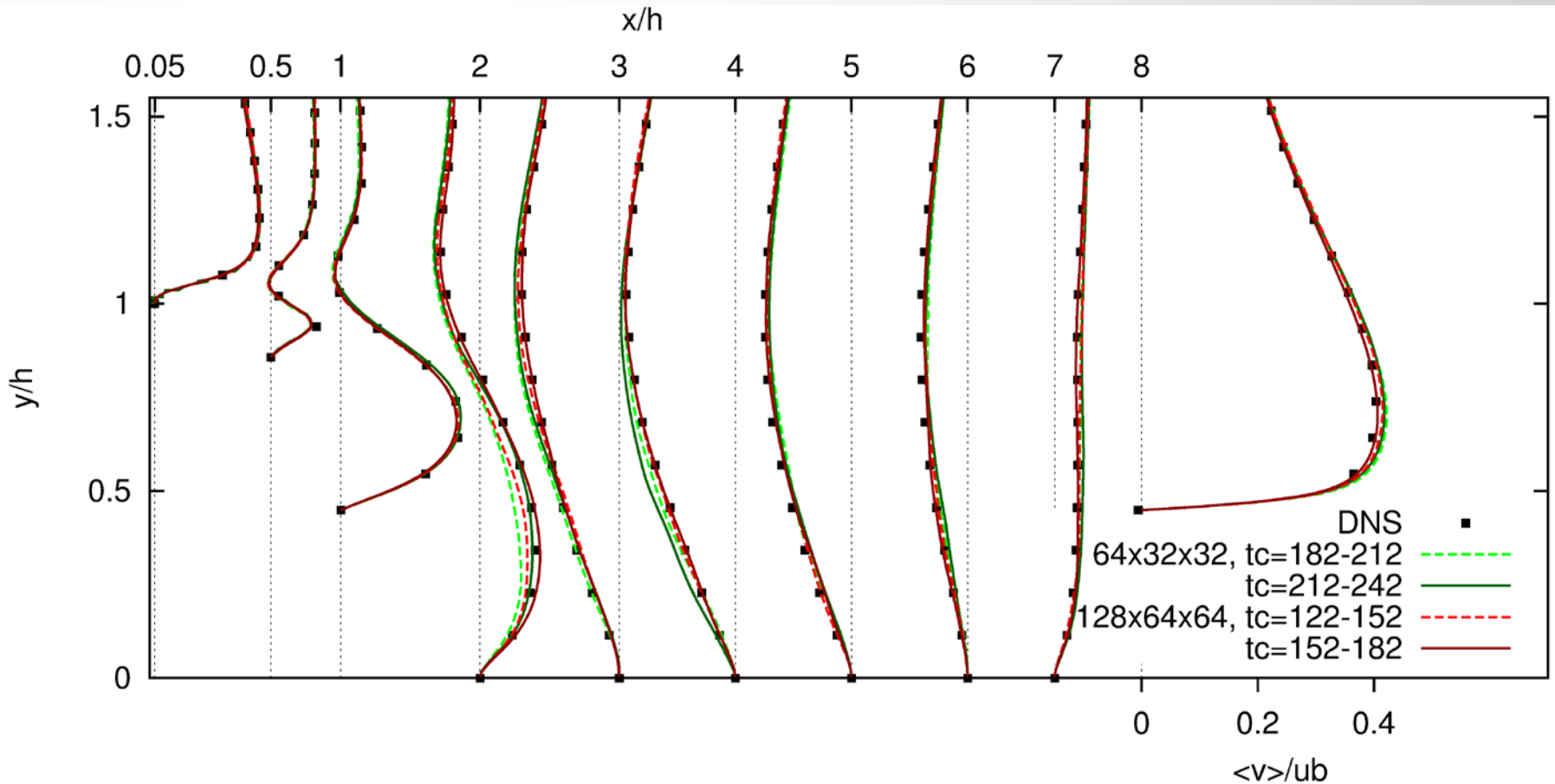
ILES for the 2D Periodic Hill test case at $Re_b=2800$



ILES for the 2D Periodic Hill test case at $Re_b=2800$



ILES for the 2D Periodic Hill test case at $Re_b=2800$



Channel flow, $Re_\delta = 6875$, $Re_\tau(DNS)=392.24$: Wall-resolved ILES

Prescribed data:

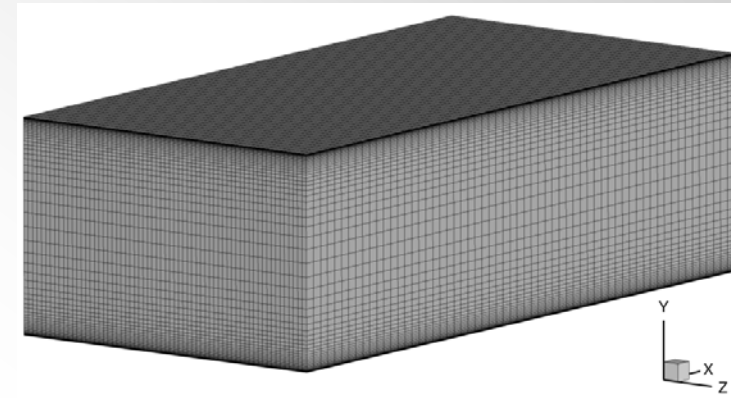
- Bulk Reynolds number $Re_\delta = U_{bulk} \cdot \delta / \nu$ and $M=0.1$

Measure quality of the (time-averaged) solution

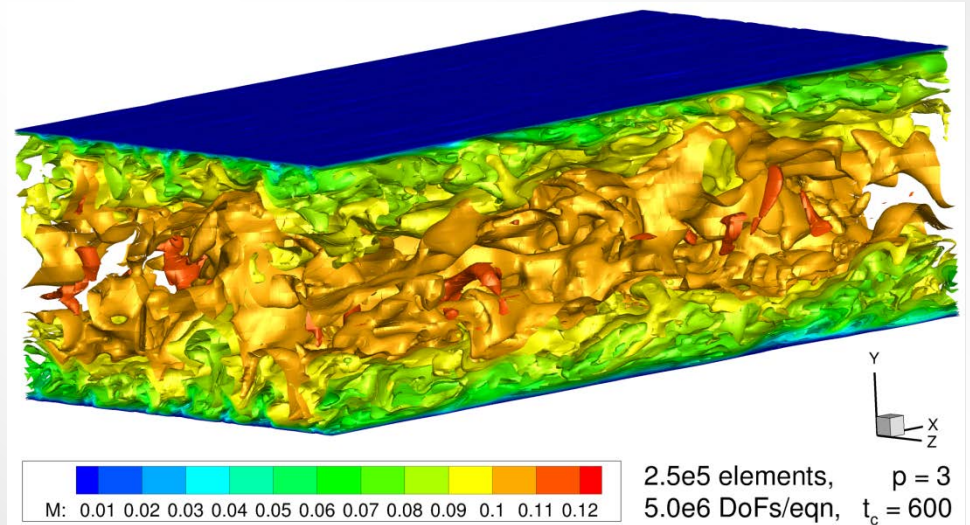
- by comparing against DNS data:
 - friction Reynolds number Re_τ
 - near-wall velocity profile $u^+(y^+)$

Computational mesh (gen. for hybrid RANS/LES [*]):

- $61 \times 64 \times 64 = 249856$ elements
- $\Delta x^+ = 41.15$, $\Delta y^+ = 0.78$, $\Delta z^+ = 19.61$

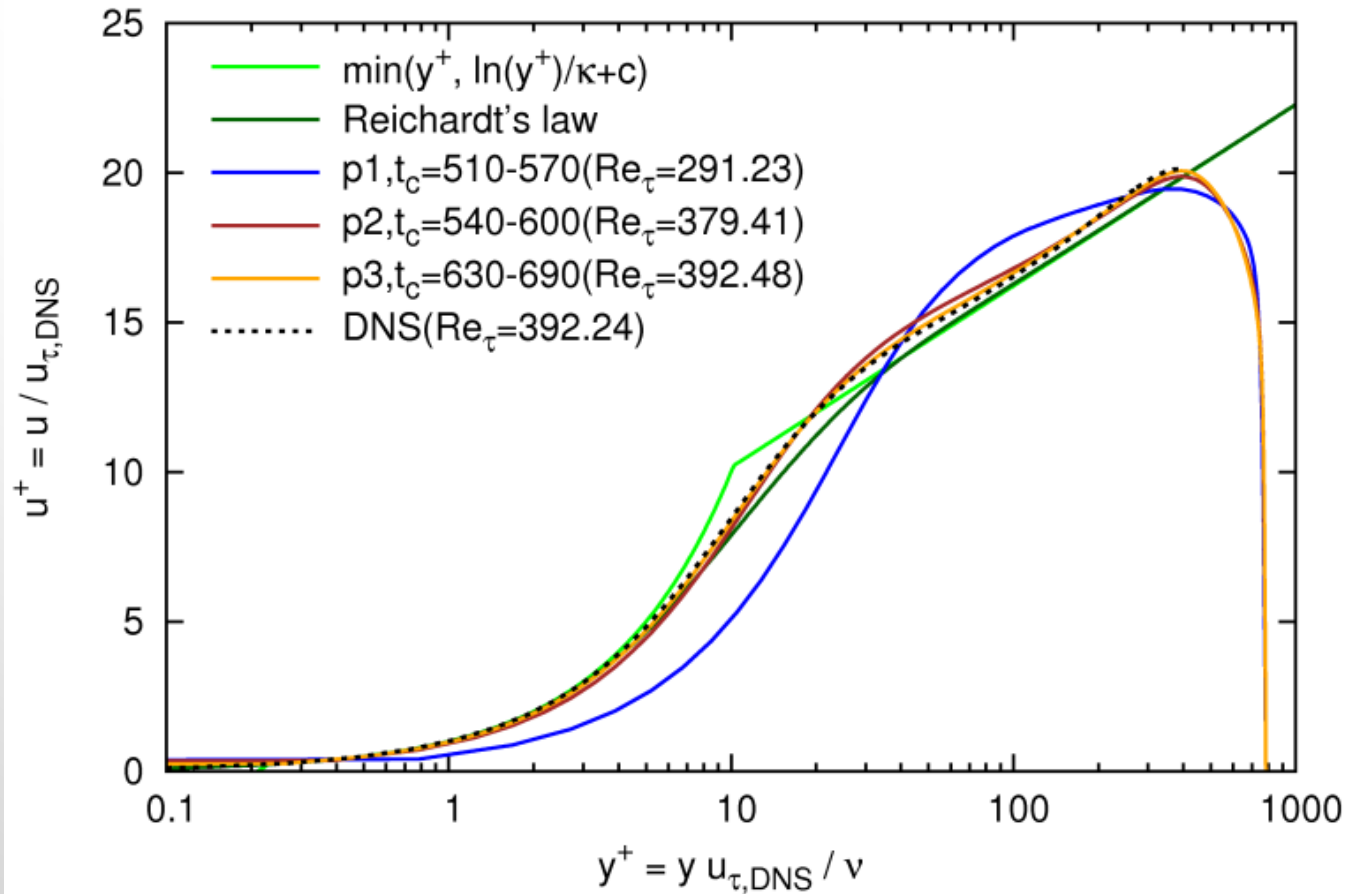


p	DoFs/eqn	T_c	Re_τ
1	1.0 M	0 - 420 420 - 450	297.65
2	2.5 M	450 - 510 510 - 540	380.20
3	5.0 M	540 - 570 570 - 600 600 - 630	392.30 391.41

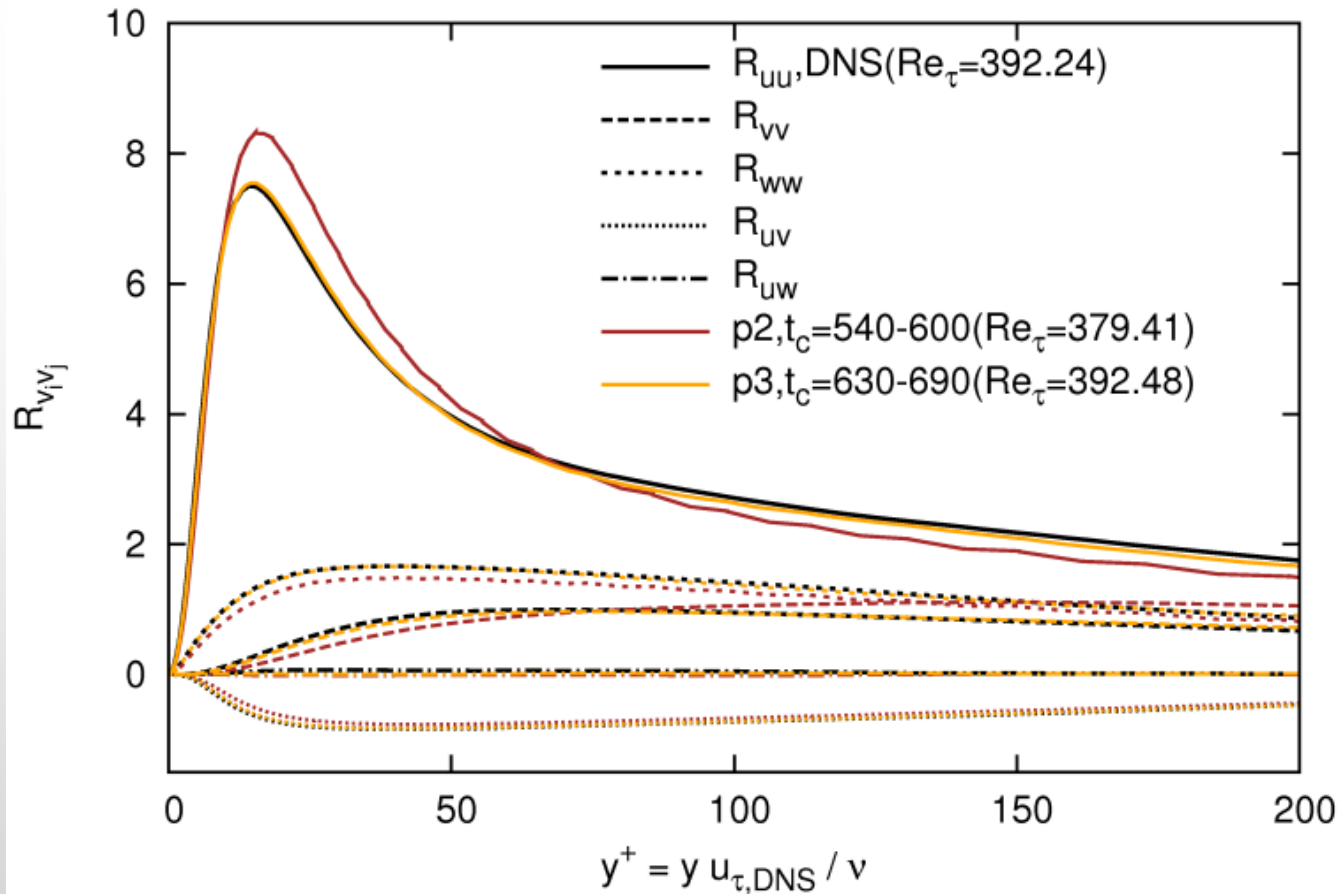


[*] Probst, Löwe, Reuß, Knopp, Kessler. AIAA Journal, vol. 54, issue 10, pp. 2972-2987, 2016.

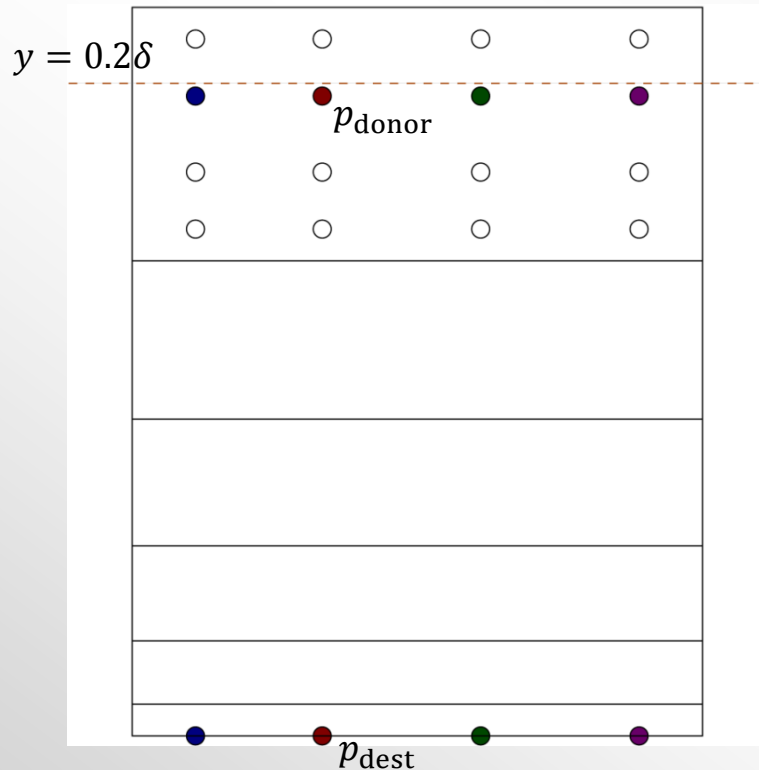
Channel flow, $Re_\delta = 6875$, $Re_\tau(DNS)=392.24$: Wall-resolved ILES



Channel flow, $Re_\delta = 6875$, $Re_\tau(\text{DNS})=392.24$: Wall-resolved ILES



A wall-stress-model approach



- For each boundary face integration point p_{dest} :
- Find a point p_{donor} normal to the wall in a distance of (approx.) $y=0.2\delta$.
 - From the solution (instantaneous flow field) at point p_{donor} take
 - tangential velocity $\mathbf{v}_t = (I - \mathbf{n} \otimes \mathbf{n}) \mathbf{v}$
 - density ρ , kinematic viscosity ν , and
 - distance $y = \text{dist}(p_{\text{donor}}, p_{\text{dest}})$.
 - Solve $u^+(y^+) = |\mathbf{v}_t|/u_\tau$ with $y^+ = yu_\tau/\nu$, i.e.

$$F(u_\tau) = |\mathbf{v}_t|/u_\tau - u^+(y u_\tau/\nu) = 0, \quad \text{for } u_\tau.$$
 - Compute wall shear stress $\tau_w = \rho u_\tau^2$.
 - In p_{face} apply slip-wall bc ($\mathbf{v} \cdot \mathbf{n} = 0$) and a viscous numerical flux $\mathbf{n} \cdot \mathbf{F}^v$ with prescribed τ_w :

Given the normal viscous flux

$$\mathbf{n} \cdot \mathbf{F}^v(\mathbf{u}, \nabla \mathbf{u}) = (0, (\tau \mathbf{n})_i, \mathbf{n} \cdot (\tau \mathbf{v}) + K \mathbf{n} \cdot \nabla T)$$

we split $(\tau \mathbf{n})_i = \tau_{ij} n_j$ into a wall normal and wall tangential part as follows

$$(\tau \mathbf{n}) = (\tau \mathbf{n})_n + (\tau \mathbf{n})_t \quad \text{with } (\tau \mathbf{n})_t = (I - \mathbf{n} \otimes \mathbf{n}) (\tau \mathbf{n}),$$

replace $(\tau \mathbf{n})_t$ by $(\tau \mathbf{n})_t^{\text{wm}} = -\tau_w \hat{\mathbf{v}}_t$ and use the adiabatic condition $K \mathbf{n} \cdot \nabla T = 0$.

Near-wall velocity profiles

$u(y)$ scaled with the friction velocity u_τ and the kinematic viscosity ν :

$$u^+(y^+) \quad \text{with} \quad u^+ = u/u_\tau \quad \text{and} \quad y^+ = y u_\tau/\nu$$

Algebraic near-wall velocity profiles:

- Logarithmic law-of-wall (log-law): $u^+(y^+) = \min(y^+, \ln(y^+)/\kappa + c)$
 - Von Karman constant $\kappa \in [0.38, 0.41]$ and $c \in [4.1, 5.1]$
 - Take $\kappa=0.38$ and $c=4.1$ [Österlund et al., 2000]
- Reichardt's law-of-wall: $u^+(y^+) = \ln(1 + \kappa y^+)/\kappa + A(1 - e^{-y^+/B} - y^+/B e^{-y^+/C})$
 - $A \in [6.6, 7.8]$, $B = 11$, $C = 3$
 - Take $A = c - \ln(\kappa)/\kappa$ [Frere, de Wiart, Hillewart et al., 2017]
- Spalding's (inverse) law-of-wall: $y^+(u^+)$

„Exact“ near-wall velocity profile:

- Moser, Kim, Mansour(1999): DNS of turbulent channel flow up to $Re_\tau=590$.

Near-wall velocity profiles

$u(y)$ scaled with the friction velocity u_τ and the kinematic viscosity ν :

$$u^+(y^+) \quad \text{with} \quad u^+ = u/u_\tau \quad \text{and} \quad y^+ = y u_\tau/\nu$$

Algebraic near-wall velocity profiles:

- Logarithmic law-of-wall (log-law): $u^+(y^+) = \min(y^+, \ln(y^+)/\kappa + c)$
 - Von Karman constant $\kappa \in [0.38, 0.41]$ and $c \in [4.1, 5.1]$
 - Take $\kappa=0.38$ and $c=4.1$ [Österlund et al., 2000]
- **Reichardt's law-of-wall:** $u^+(y^+) = \ln(1 + \kappa y^+)/\kappa + A(1 - e^{-y^+/B} - y^+/B e^{-y^+/C})$
 - $A \in [6.6, 7.8]$, $B = 11$, $C = 3$
 - Take $A = c - \ln(\kappa)/\kappa$ [Frere, de Wiart, Hillewart et al., 2017]
- Spalding's (inverse) law-of-wall: $y^+(u^+)$

„Exact“ near-wall velocity profile:

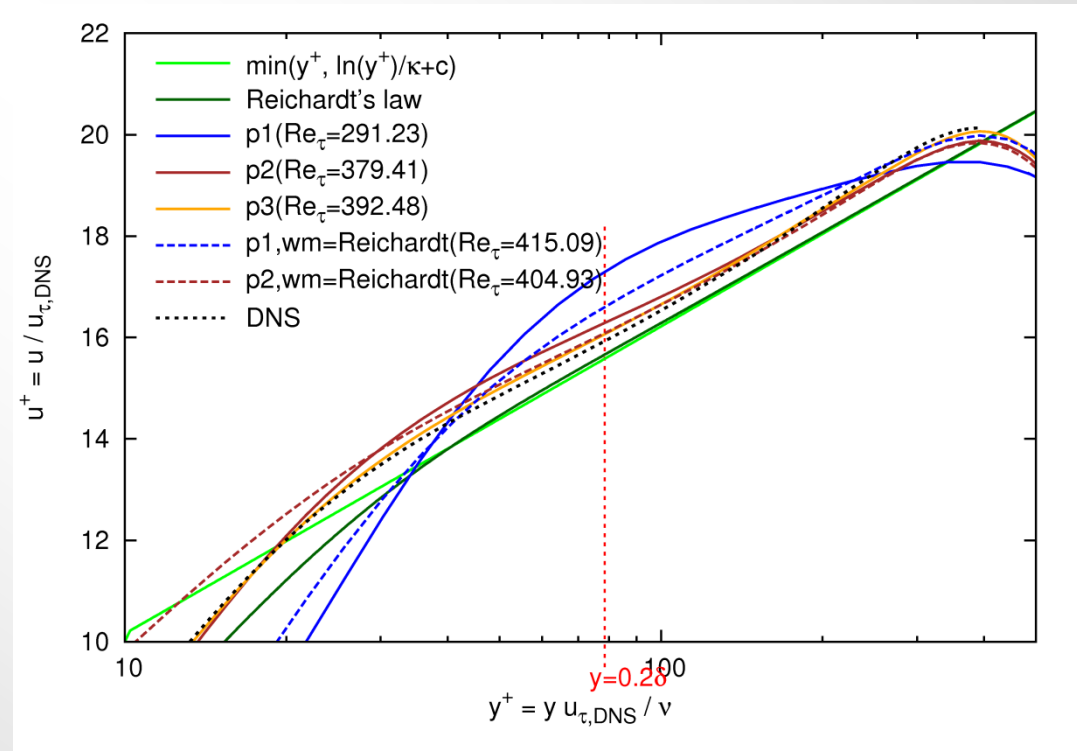
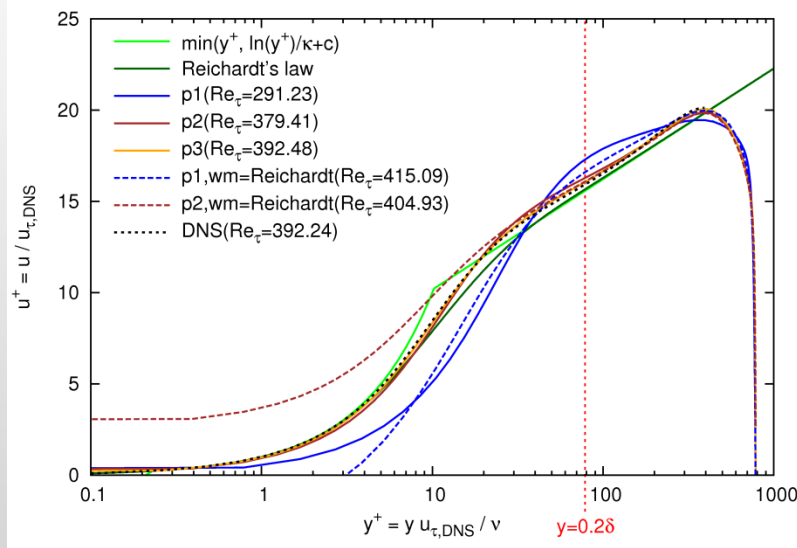
- **Moser, Kim, Mansour(1999): DNS** of turbulent channel flow up to $Re_\tau=590$.

Channel flow, $Re_\delta = 6875$, $Re_\tau(\text{DNS})=392.24$: Wall-modelled ILES vs. wall-resolved ILES

p	DoFs/ eqn	ILES Re_τ	WM-ILES	WM-ILES	DNS [Moser et al.] $Re_{\tau,DNS}$
			$u^+(y^+)=\text{Reichardt}$ Re_τ	$u^+(y^+)=\text{DNS data}$ Re_τ	
1	1.0e6	293.08 (-25.3%)	415.24 (5.9%)	408.98 (4.3%)	392.24
		291.23 (-25.8%)	418.81 (6.8%)	409.89 (4.5%)	
			415.09 (5.8%)	408.47 (4.1%)	
2	2.5e6	379.88 (-3.2%)	403.75 (2.9%)	400.42 (2.1%)	
		379.41 (-3.3%)	404.93 (3.2%)	399.78 (1.9%)	
3	5.0e6	391.86 (-0.1%)			
		392.48 (0.06%)			

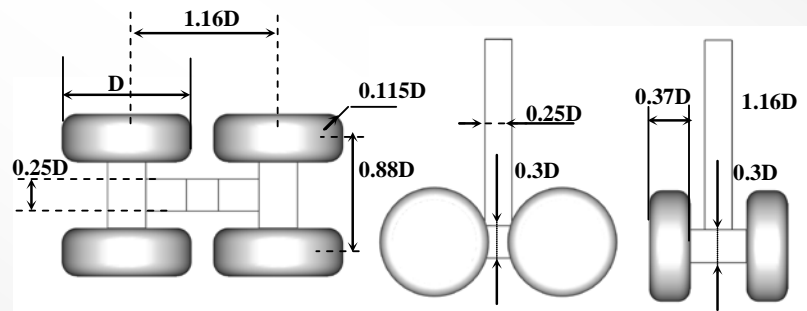
Table 4: Channel flow at $Re_\delta = 6875$: Comparison of friction Reynolds numbers for ILES and two versions of WM-ILES (once $u^+(y^+)$ is given by Reichardt's law and once given by DNS data) compared to $Re_{\tau,DNS}$ [Moser et al., 1999]. Re_τ values are computed from solutions averaged over 60 CTU (for ILES) and 120 CTU (for WM-LES). Deviations of computed Re_τ values from $Re_{\tau,DNS}$ are given as percentages.

Channel flow, $Re_\delta = 6875$, $Re_\tau(\text{DNS})=392.24$: Wall-modelled ILES vs. wall-resolved ILES



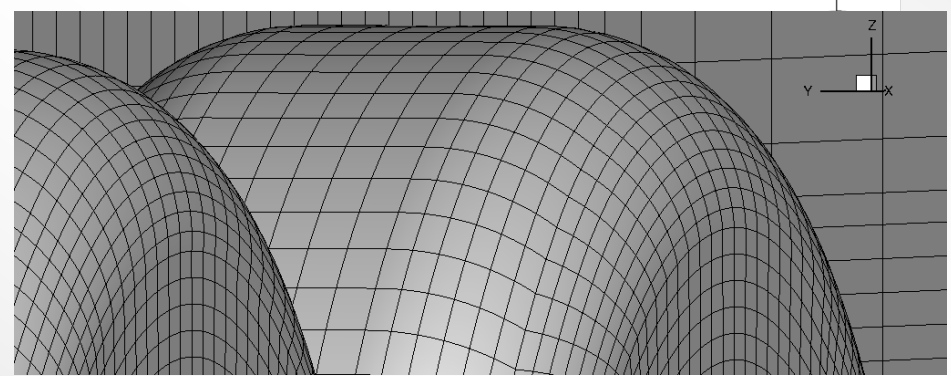
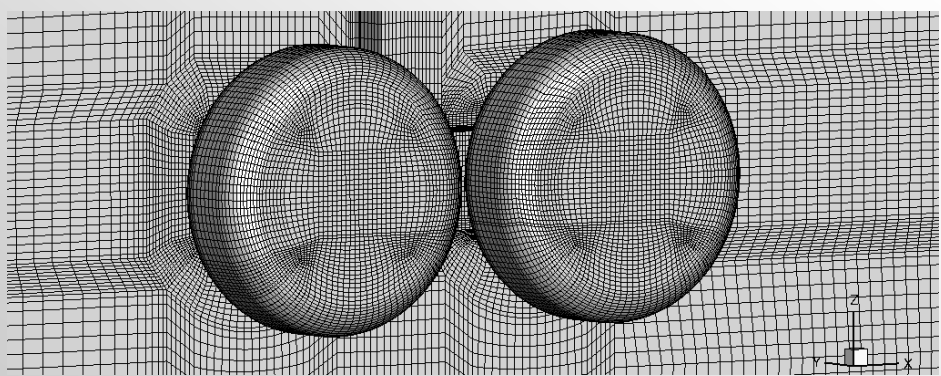
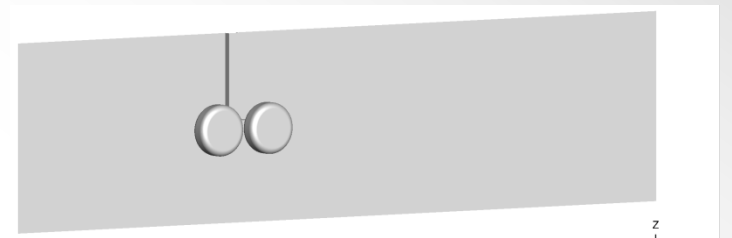
Boeing Rudimentary landing gear

$U=40\text{m/s}$, ($M\approx 0.12$), $Re=UD/v\approx 10^6$



Grids derived from structured grid (ATAAC)

- coarse(115k), medium(924k), fine(7.4M)



medium quadratic grid with 924k elements

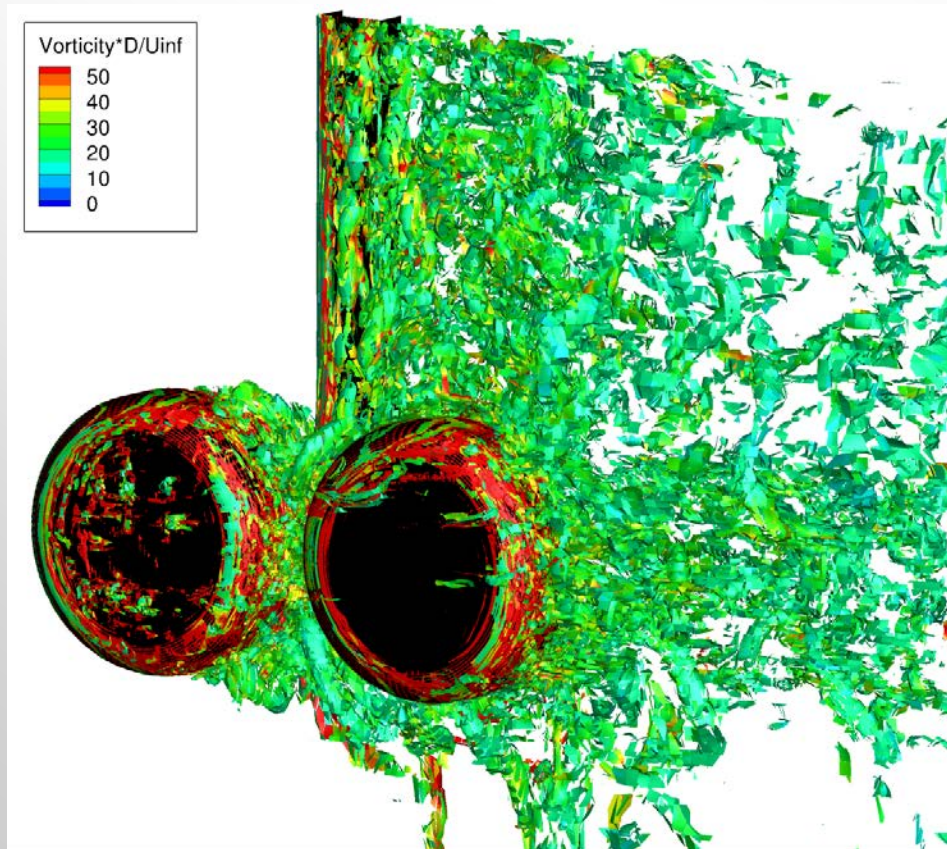
ILES for the Boeing RLG

For $p=2$ on medium grid:

- ERK-4: 50e6 steps/CTU
- SDIRK-4: 200 steps/CTU

Computational time(ERK/SDIRK)=100*

grid	# el	p	DoFs/eqn	Δt_c	t_c
coarse	115 K	1	0.5 M	0.01	0-30
medium	924 K	1	3.7 M	0.01	30-60
		2	9.2 M	0.005	60- 66.6



Medium quadratic grid
 $p=2$ (3rd order DG)
 local Lax-Friedrichs flux

Instantaneous flow field at $t_c=65.6$:

- Iso-surfaces of Q criterion
 $Q (D/U_\infty)^2=50$
 colored with the vorticity magn.

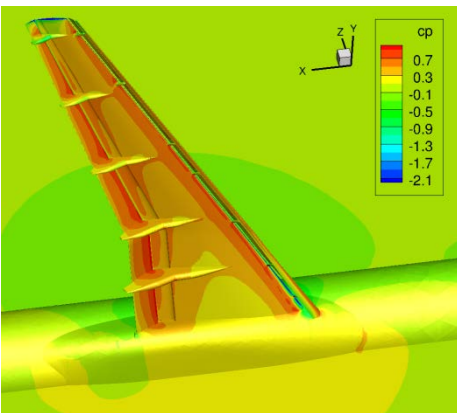
Computation broke after $t_c=66.6$

Next steps: Use

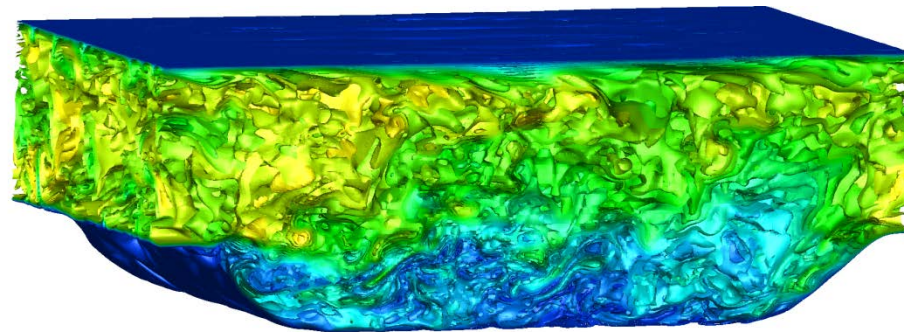
- BCs based on Riemann invariants
- Sponge layer near outflow?
- WM-ILES

Summary

- DG discretization of equations, integral quantities and local quantities
- Details on discretization settings and results for RANS and ILES:
 - RANS and Wilcox- $k\omega$ for the DLR-F11 high lift configuration
 - Computational time(ERK/SDIRK)=2.5(TGV), 100*(Boeing RLG)
 - **Wall-resolved ILES** for 2D periodic hill and channel flow with results very close to DNS data
 - **Wall-modelled ILES** for channel flow with significant improvement over ILES
- Current state of ILES computations for the Boeing rudimentary landing gear

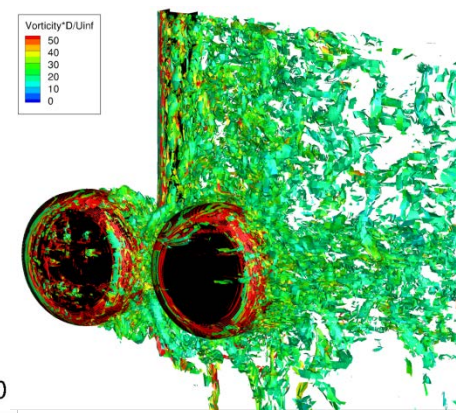


RANS- $k\omega$ with $p=2$



M : 0 0.01 0.02 0.03 0.04 0.05 0.06 0.07 0.08 0.09 0.1 0.11 0.12 0.13 0.14 0.15
 $p = 3$ $128 \times 64 \times 64 = 524288$ cells
 $tc = 182.000$

ILES with $p=3$



ILES with $p=2$

